

Dispersion of double-slot microring resonators in optical buffer

Chuan WANG, Xiaoying LIU (✉), Peng ZHOU, Peng LI, Jia DU

School of Optical and Electronic Information, Huazhong University of Science and Technology, Wuhan 430074, China

© Higher Education Press and Springer-Verlag Berlin Heidelberg 2015

Abstract In the optical packet switching network, optical buffer is an important device. Microring resonator optical buffers provide good delay performance and flexibility in design. By cascading multiple microring resonators, higher delay-bandwidth product is obtained, but the requirements of high integration and low dispersion are hard to satisfy simultaneously. Double-slot waveguide was proposed to construct highly integrated racetrack microring resonators in this study. Based on dispersion analysis of the thickness of each layer of a waveguide, the structure of waveguide was optimized to reach flat and low dispersion. Average dispersions of straight and 3 μm bend waveguides were 5.1 ps/(nm·km) and 4.4 ps/(nm·km), respectively. Besides, the additional loss from coupling was greatly reduced when applying proper relative displacement between straight and bend waveguides. Theoretical and design basis provided in this paper will help to develop multi-microring optical buffers in the future.

Keywords microring, optical buffer, double-slot waveguide

1 Introduction

Modern optical communication networks are developing fast toward high-speed, high-capacity and high integration. The requirements proposed for optoelectronic devices are buffering and routing of optical signals on-chip. Optical buffer is a key component in switching node of all-optical communication, which needs to meet the demands of both input signal for bandwidth and optical network for delay. Optical microring has become a research hotspot as it is used to construct lasers, filters, modulators, switches and buffers, which is conducive to on-chip system integration

[1–6]. Optical buffers based on microring resonators slow down the speed of light through making light transport back and forth in special resonator structure with good flexibility and tenability [7–10].

The main design goals of microring resonator optical buffers are large delay, large bandwidth, low dispersion, low loss and high integration. In single-ring optical buffer, the product of delay and the delay-bandwidth have an inherent theoretical upper limit [11]. To increase the delay-bandwidth, multi rings are cascaded according to the Vernier effect [2,10,12], while the device footprint would be too large as the number of rings increases. In 2006, Poon et al. made a 12-ring buffer with 110–140 ps delay and 60 μm ring radius [13]. Cooper et al. integrated 235 rings on silicon on insulator (SOI) in 2010, each ring has an average radius of 90 μm [14]. The dispersion characteristics will be deteriorated significantly if smaller radius is implemented on microring with ordinary strip waveguide structure. On the other hand, the mode distribution will be extended outwards and cause energy leak and big transmission loss when the waveguide is at highly bend state.

In 2004, Almeida et al. first proposed the concept of slot waveguide [15]. Between two high-index waveguide layers, there is a waveguide slot of tens of nanometers with material of low index of refraction. This kind of waveguide structure can provide strong optical field concentration with high optical confinement and power density in small volume [16,17]. Then, there are many research reports showed that the slot waveguide has excellent controllable dispersion and nonlinearity characteristics. By properly modifying structural parameters, the waveguide device's dispersion and nonlinearity characteristics were optimized to achieve a high degree of freedom in design [18–22]. And in the bend waveguide case, appropriate structural parameters of multi-slot waveguide enable lower transmission loss [23].

In this paper, we simulated and analyzed the double-slot microring resonator's dispersion characteristics under

different structural parameters to minimize the dispersion and the transmission loss over communication bandwidth, and provide theoretical basis for designing multi-microring optical buffer with excellent performance.

2 Structure of optical buffer

Figure 1(a) shows the structure of racetrack microring resonator and the basic component of optical buffer, in which there are two straight tracks of length l_c and two semicircular tracks of radius R . The coupling area (as shown in the dashed box section) between the lower straight track in the microring and the adjacent straight waveguide is formed, the coupling gap is g .

We used double-slot waveguide, as shown in Figs. 1(b) and 1(c), for both straight and curved waveguides in racetrack microring. The double-slot waveguide is formed by adding two horizontal slot layers of low index in high index waveguide. The waveguide's material is silicon and the slot's material is silica. The $2\ \mu\text{m}$ waveguide substrate is silica, and the cladding is air. The waveguide's structural parameter was simulated using finite difference time domain (FDTD) method to compute dispersion, and Sellmeier equations were used in different materials. There are 6 structural parameters in a double-slot waveguide: the width w , thicknesses of top, middle and bottom silicon waveguide layers $h_{\text{wg-u}}$, $h_{\text{wg-c}}$ and $h_{\text{wg-d}}$, thicknesses of upper and lower slot waveguide layers $h_{\text{slot-u}}$ and $h_{\text{slot-d}}$.

3 Principle of dispersion tailoring in double-slot waveguide

3.1 Waveguide layers thicknesses influence on dispersion

In slot waveguide, the thickness of each layer will affect the effective index of the waveguide and the waveguide

dispersion. As reference parameters, we chose the waveguide width of $w = 600\ \text{nm}$, three layers of silicon thickness $h_{\text{wg-u}} = 100\ \text{nm}$, $h_{\text{wg-c}} = 384\ \text{nm}$ and $h_{\text{wg-d}} = 112\ \text{nm}$, two layers of slot thickness $h_{\text{slot-u}} = 42\ \text{nm}$ and $h_{\text{slot-d}} = 72\ \text{nm}$. To analyze the impact of the thickness of waveguide layers, each simulation group changed one parameter of five from top to bottom layer. The dispersion results are shown in Figs. 2–6.

As can be seen from the simulation results, the dispersion decreases when top or bottom silicon layer thickness increases. The dispersion at wavelength $1.55\ \mu\text{m}$ will decrease from 200 to $-200\ \text{ps}/(\text{nm}\cdot\text{km})$ as the thickness of top silicon layer increased by 40 nm, and it will also drop from 100 to $-100\ \text{ps}/(\text{nm}\cdot\text{km})$ in the simulation case of bottom silicon layer. The influence rates are 10 and 5 $\text{ps}/(\text{nm}^2\cdot\text{km})$, respectively. The top silicon layer has small influence on the flatness, as the communication band lies in the flat part of the dispersion curve, while when the bottom silicon layer gets thicker, the flatness of communication band is much worse and the dispersion slope will decrease.

The middle silicon waveguide and the lower slot have similar influences on dispersion. When the thickness increased by 45 nm, the dispersion at wavelength $1.55\ \mu\text{m}$ will increase from 50 to 150 $\text{ps}/(\text{nm}\cdot\text{km})$ in the simulation case of middle silicon waveguide, and from 0 to 300 $\text{ps}/(\text{nm}\cdot\text{km})$ in the simulation case of lower slot. The influence rates are 4.4 and 6.7 $\text{ps}/(\text{nm}^2\cdot\text{km})$, respectively, the lower slot has a bigger effect on dispersion. These two parameters have so little influence on the dispersion slope in communication band that we can ignore them in the process of the structural optimization in order to simplify.

Upper slot has a complex influence. As the thickness increased from 20 to 70 nm, the zero-dispersion-slope-wavelength got smaller, zero-dispersion-wavelength (ZDW) first increased and then decreased. The reason is that the mode distribution of the waveguide is close to this slot. This structural parameter can be used to fix the dispersion slope during the optimization process.

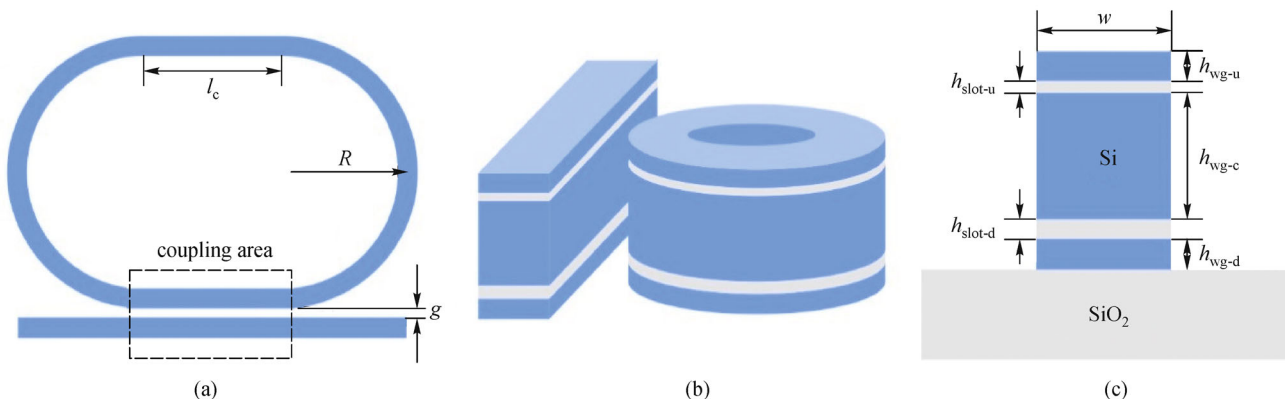


Fig. 1 (a) Structure and (b) space diagram of microring resonator; (c) structure of double-slot waveguide

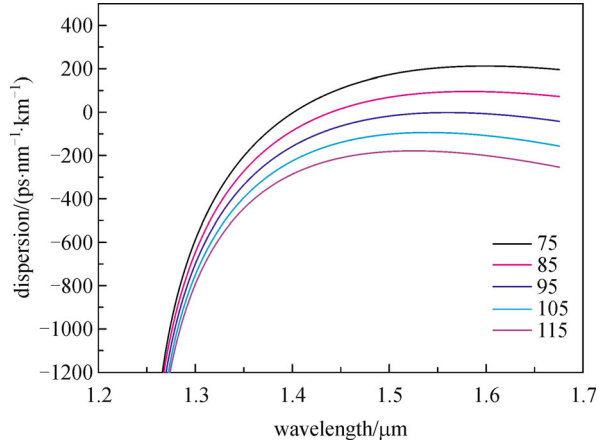


Fig. 2 Dispersion tailored by thickness (nm) of upper waveguide

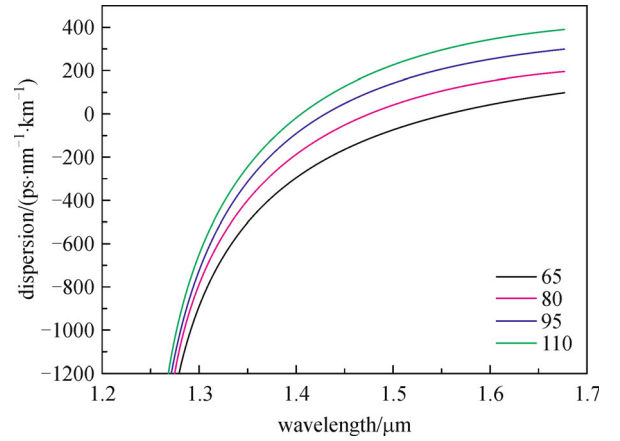


Fig. 5 Dispersion tailored by thickness (nm) of lower slot

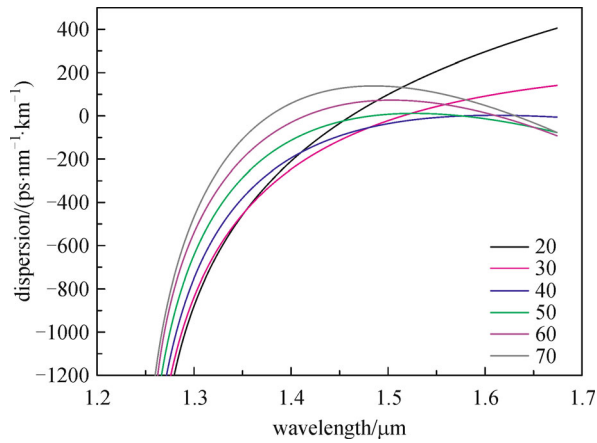


Fig. 3 Dispersion tailored by thickness (nm) of upper slot

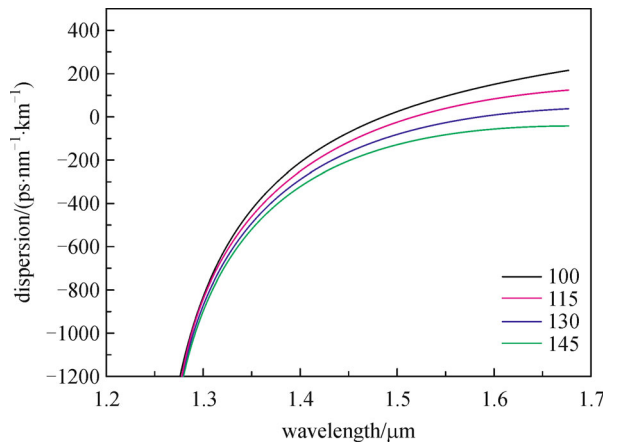


Fig. 6 Dispersion tailored by thickness (nm) of lower waveguide

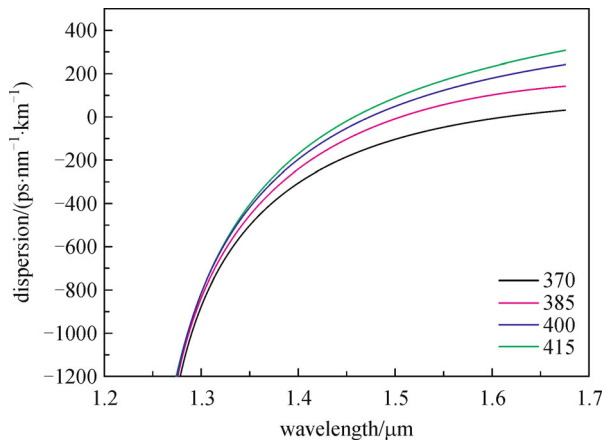


Fig. 4 Dispersion tailored by thickness (nm) of middle waveguide

3.2 Waveguide radius' influence on dispersion

To analyze the dispersion of the semicircular waveguide of

the microring resonator, we examined the impact of the bending radius on the dispersion in this section. The waveguide remains in the reference parameters structure, and the waveguide's bending radius was changed from no bend to 10, 7.5, 5, 3 and 2 μm , making the waveguide bending more. The simulation results are shown in Fig. 7. When the bending radius was larger than 5 μm , the dispersion profile was close to the profile of straight waveguide. The dispersion profile was decreased significantly as the bending radius got smaller and the dispersion profile was no longer horizontal. In the case of 3 μm , the dispersion at wavelength 1.55 μm was $-400 \text{ ps}/(\text{nm} \cdot \text{km})$.

4 Structure optimization of double-slot waveguide

4.1 Straight waveguide structure optimization

To realize zero dispersion on broadband, we optimized the waveguide structure and got a set of optimal structure

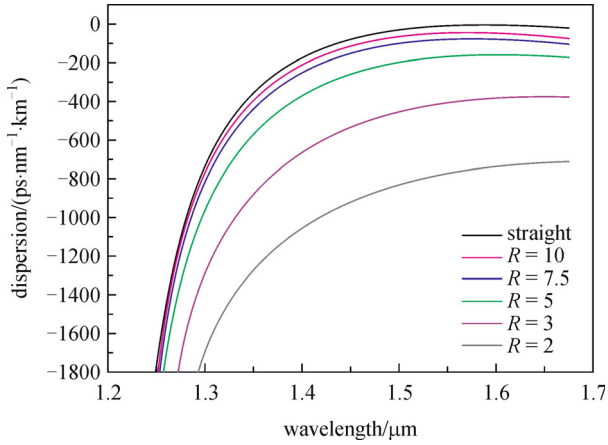


Fig. 7 Dispersion tailored by radius (μm) of bend waveguide

parameters: $h_{\text{wg-u}} = 100 \text{ nm}$, $h_{\text{wg-c}} = 384 \text{ nm}$, $h_{\text{wg-d}} = 112 \text{ nm}$, $h_{\text{slot-u}} = 42 \text{ nm}$ and $h_{\text{slot-d}} = 72 \text{ nm}$. The dispersion of this structure is shown in Fig. 8. As shown, the dispersion at wavelength $1.53\text{--}1.63 \mu\text{m}$ is $-14\text{--}0.5 \text{ ps}/(\text{nm}\cdot\text{km})$, the average was $-5.1 \text{ ps}/(\text{nm}\cdot\text{km})$, which was very close to zero and the dispersion flatness (dispersion range divided by bandwidth) was $0.135 \text{ ps}/(\text{nm}^2\cdot\text{km})$.

4.2 Bend waveguide structure optimization

According to the analysis of the impact of each structural parameter on the dispersion, and the simulation results of bend waveguide, we need to re-simulate the bend waveguide structure to make its dispersion small and get close to zero in communication band. But when the waveguide structures of straight waveguide and bend waveguide are different, the waveguide modes will be different which will cause additional loss in mode coupling. To reduce this loss, during the optimization process, the overlap ratio between these two modes should be as high as possible. The previous simulation results showed that increasing the thickness of lower slot or decreasing the thickness of bottom silicon can lift the dispersion profile and compensate the profile's sinking caused by bending. In addition, if we adjust the thicknesses of these two layers at the same time and equate the adjustment amounts, then we can keep the position of middle silicon layer unchanged, which will improve the overlap ratio of modes.

As an example, we chose the bending waveguide radius of $3 \mu\text{m}$ to make a structural optimization. The optimization results were: $h_{\text{wg-u}} = 100 \text{ nm}$, $h_{\text{wg-c}} = 384 \text{ nm}$, $h_{\text{wg-d}} = 82 \text{ nm}$, $h_{\text{slot-u}} = 60 \text{ nm}$ and $h_{\text{slot-d}} = 102 \text{ nm}$. Optimized structures of straight waveguide and bend waveguide are shown in Fig. 9, and the middle layer silicon's position was unchanged.

The dispersions of bend waveguide before and after optimization are shown in Fig. 10. We can see that the

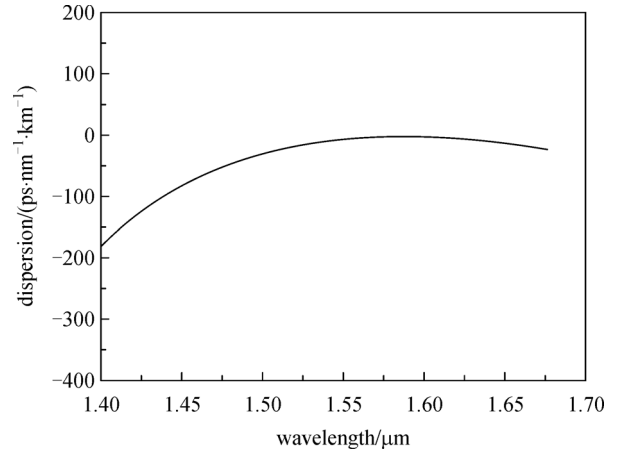


Fig. 8 Dispersion of straight double-slot waveguide

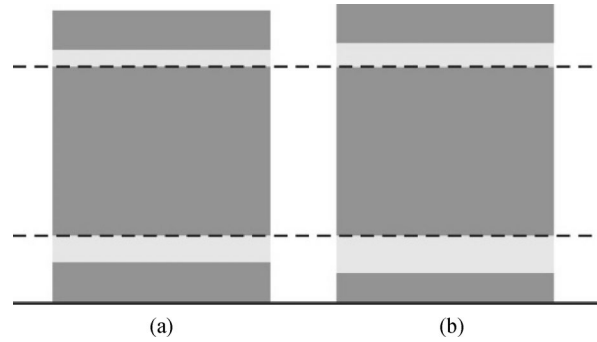


Fig. 9 Keep the middle layer unchanged of (a) straight and (b) bend waveguide structure

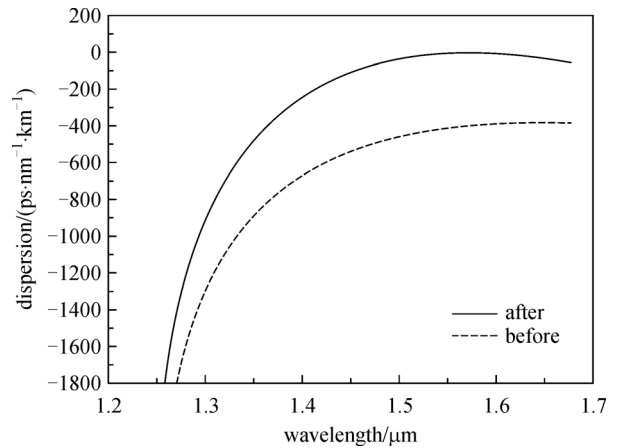


Fig. 10 Dispersion of bend waveguide before and after optimization

dispersion after optimization was much more close to zero, which was $-14\text{--}2.9 \text{ ps}/(\text{nm}\cdot\text{km})$ at $1.53\text{--}1.63 \mu\text{m}$ wavelength. The average of dispersion was $-4.4 \text{ ps}/(\text{nm}\cdot\text{km})$, and the dispersion flatness was $0.169 \text{ ps}/(\text{nm}^2\cdot\text{km})$.

4.3 Modes mismatch

Mode distributions of straight and $3\ \mu\text{m}$ bend waveguide are shown in Fig. 11, the transmission wavelength was $1.55\ \mu\text{m}$. Compared to straight waveguide, the mode of bend waveguide had a certain offset, the value of offset is s , and the offset orientation is outward of bending. The overlap ratio can be simulated and the additional loss was calculated as $0.199\ \text{dB}$. To reduce the additional loss, we moved the straight track in the microring outwards a distance of s , as shown in Fig. 12, and made two modes align at center, which will improve the overlap ratio and the coupling efficiency. Simulation results demonstrated that when the move distance, s is $54\ \text{nm}$, the overlap ratio reach the maximum and the additional loss is $0.0224\ \text{dB}$, lowered by 89% than before moving.

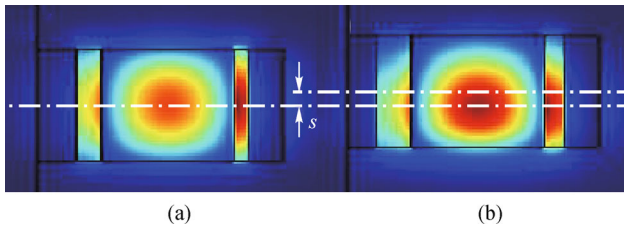


Fig. 11 Mode distributions at $1.55\ \mu\text{m}$ of (a) straight and (b) bend waveguide

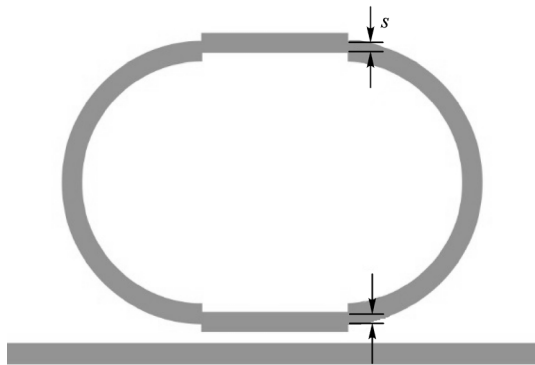


Fig. 12 Schematic of waveguide offset

5 Conclusions

In this paper, we simulated and analyzed the double-slot silicon waveguide using FDTD method. Considering the common C and L communication bands, the dispersion of straight waveguide after structural optimization was $-5.1\ \text{ps}/(\text{nm}\cdot\text{km})$ and the flatness of dispersion was $0.135\ \text{ps}/(\text{nm}^2\cdot\text{km})$; the dispersion of $3\ \mu\text{m}$ bend waveguide after structural optimization was $-4.4\ \text{ps}/(\text{nm}\cdot\text{km})$ and the flatness was $0.169\ \text{ps}/(\text{nm}^2\cdot\text{km})$, both meet the requirements of low and flat dispersion. As for other bending radius of waveguide, similar optimization can be

done. Simulation results showed that fixing the mode distribution offset of bend waveguide can greatly reduce the additional loss of mode coupling. When moving straight waveguide outwards $54\ \text{nm}$, the additional loss reduced from $0.199\ \text{dB}$ to $0.0224\ \text{dB}$, lowered by 89% . We have shown that in microring resonators with small semicircular radius and small footprint, structural optimization can flatten and lower the dispersion in communication and relatively low additional loss. Such capability of tailoring waveguide properties could provide important basis in multi-ring resonators optical buffer.

Acknowledgements This work was supported by the National Natural Science Foundation of China (Grant No. 61107051) and National High-tech R&D Program (No. SS2012AA010407).

References

- Willner A E, Zhang L, Yang J Y. Micro-resonator devices and optical broadband access application. In: Proceedings of the International Society for Optics and Photonics, (OPTO). 2011, 795803
- Bogaerts W, De Heyn P, Van Vaerenbergh T, De Vos K, Kumar Selvaraja S, Claes T, Dumon P, Bienstman P, Van Thourhout D, Baets R. Silicon microring resonators. *Laser & Photonics Reviews*, 2012, 6(1): 47–73
- Xia F, Sekaric L, Vlasov Y. Ultracompact optical buffers on a silicon chip. *Nature Photonics*, 2007, 1(1): 65–71
- Cao T T, Zhang L B, Fei Y H, Cao Y M, Lei X, Chen S W. Design of a high-speed silicon electro-optical modulator based on an add-drop micro-ring resonator. *Acta Physica Sinica*, 2013, 62(19): 194210 (in Chinese)
- Zhang X, Li Z Q, Tong K. A cross bus single microring electro-optical switch with U bend waveguide. *Acta Physica Sinica*, 2014, 63(9): 094207 (in Chinese)
- Ren G H, Chen S W, Cao T T. Theoretical analysis of a thermal-optical tunable filter based on Vernier effect of cascade microring resonators. *Acta Physica Sinica*, 2012, 61(3): 034215 (in Chinese)
- Fontaine N K, Yang J, Pan Z, Chu S, Chen W, Little B E, Ben Yoo S. Continuously tunable optical buffering at $40\ \text{Gb/s}$ for optical packet switching networks. *Journal of Lightwave Technology*, 2008, 26(23): 3776–3783
- Shinobu F, Ishikura N, Arita Y, Tamanuki T, Baba T. Continuously tunable slow-light device consisting of heater-controlled silicon microring array. *Optics Express*, 2011, 19(14): 13557–13564
- Morichetti F, Melloni A, Breda A, Canciamilla A, Ferrari C, Martinelli M. A reconfigurable architecture for continuously variable optical slow-wave delay lines. *Optics Express*, 2007, 15(25): 17273–17282
- Boeck R, Chrostowski L, Jaeger N A. Thermally tunable quadruple Vernier racetrack resonators. *Optics Letters*, 2013, 38(14): 2440–2442
- Khurgin J B. Optical buffers based on slow light in electromagnetically induced transparent media and coupled resonator structures: comparative analysis. *Journal of the Optical Society of America B*,

- 2005, 22(5): 1062–1074
12. Poon J K, Scheuer J, Xu Y, Yariv A. Designing coupled-resonator optical waveguide delay lines. *Journal of the Optical Society of America B*, 2004, 21(9): 1665–1673
 13. Poon J K, Zhu L, DeRose G A, Yariv A. Transmission and group delay of microring coupled-resonator optical waveguides. *Optics Letters*, 2006, 31(4): 456–458
 14. Cooper M L, Gupta G, Schneider M A, Green W M, Assefa S, Xia F, Gifford D K, Mookherjea S. Waveguide dispersion effects in silicon-on-insulator coupled-resonator optical waveguides. *Optics Letters*, 2010, 35(18): 3030–3032
 15. Almeida V R, Xu Q, Barrios C A, Lipson M. Guiding and confining light in void nanostructure. *Optics Letters*, 2004, 29(11): 1209–1211
 16. Sun R, Dong P, Feng N N, Hong C Y, Michel J, Lipson M, Kimmerling L. Horizontal single and multiple slot waveguides: optical transmission at $\lambda = 1550$ nm. *Optics Express*, 2007, 15(26): 17967–17972
 17. Yu P, Qi B, Jiang X, Wang M, Yang J. Ultrasmall- V high- Q photonic crystal nanobeam microcavities based on slot and hollow-core waveguides. *Optics Letters*, 2011, 36(8): 1314–1316
 18. Zhang L, Yue Y, Xiao-Li Y, Wang J, Beausoleil R G, Willner A E. Flat and low dispersion in highly nonlinear slot waveguides. *Optics Express*, 2010, 18(12): 13187–13193
 19. Bao C, Yan Y, Zhang L, Yue Y, Willner A E. Tailoring of low chromatic dispersion over a broadband in silicon waveguides using a double-slot design. In: *Proceedings of CLEO: QELS_Fundamental Science*. 2013, JTU4A.53
 20. Yan Y, Matsko A, Bao C, Maleki L, Willner A E. Increasing the spectral bandwidth of optical frequency comb generation in a microring resonator using dispersion tailoring slotted waveguide. In: *Proceedings of IEEE Photonics Conference (IPC)*. 2013, 230–231
 21. Zhu M, Liu H, Li X, Huang N, Sun Q, Wen J, Wang Z. Ultrabroadband flat dispersion tailoring of dual-slot silicon waveguides. *Optics Express*, 2012, 20(14): 15899–15907
 22. Sanchis P, Blasco J, Martínez A, Martí J. Design of silicon-based slot waveguide configurations for optimum nonlinear performance. *Journal of Lightwave Technology*, 2007, 25(5): 1298–1305
 23. Keivani H, Kargar A. Bending efficiency of bent multiple-slot waveguides. *Chinese Physics Letters*, 2009, 26(12): 124204



Chuan WANG received the B.S. degree in the College of Optoelectronics Science and Engineering from Huazhong University of Science & Technology, Wuhan, China, in 2012. She is currently working toward the M. E. degree in the School of Optical and Electronic Information, Huazhong University of Science & Technology. Her research includes simulation and designing of optical

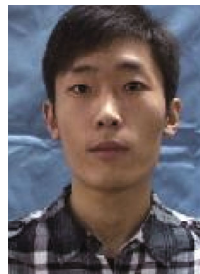
devices, such as optical buffers and system performance analyze of optical network.



Xiaoying LIU is an associate professor in the School of Optical and Electronic Information, Huazhong University of Science and Technology, Wuhan, China. She was a Postdoctoral Member of the College of Optoelectronics Science and Engineering at Huazhong University of Science and Technology in 2003. Her current research includes orthogonal frequency division multiplexing (OFDM) transmissions, advanced modulation formats, micro-ring resonators, all-optical tunable filter, optical fiber sensor and wireless sensor network.



Peng ZHOU is currently working toward the B.S. degree in the School of Optical and Electronic Information, Huazhong University of Science & Technology, Wuhan, China. His research includes optical communication system and optical devices, such as optical buffers.



Peng LI received the B.S. degree from Harbin University of Science and Technology, Harbin, China, in 2013. He is currently working toward the M.E. degree in the School of Optical and Electronic Information, Huazhong University of Science and Technology, Wuhan, China. His current research interests are coherent optical orthogonal frequency division multiplexing (CO-OFDM).



Jia DU received the B.S. degree in optical information science and technology from the East China Jiao Tong University in 2013. He is currently working toward the M.E. degree in the School of Optical and Electronic Information, Huazhong University of Science and Technology, Wuhan, China. His current research interests are coherent optical orthogonal frequency division multiplexing (CO-OFDM), optic fiber sensor.